

# Novel application of the “doubly labeled” water method: measuring CO<sub>2</sub> production and the tissue-specific dynamics of lipid and protein in vivo

Ilya R. Bederman,<sup>1</sup> Danielle A. Dufner,<sup>1</sup> James C. Alexander,<sup>2</sup> and Stephen F. Previs<sup>1,3</sup>

Departments of <sup>1</sup>Nutrition, <sup>2</sup>Mathematics, and <sup>3</sup>Medicine, Case Western Reserve University, Cleveland, Ohio

Submitted 27 July 2005; accepted in final form 14 December 2005

**Bederman, Ilya R., Danielle A. Dufner, James C. Alexander, and Stephen F. Previs.** Novel application of the “doubly labeled” water method: measuring CO<sub>2</sub> production and the tissue-specific dynamics of lipid and protein in vivo. *Am J Physiol Endocrinol Metab* 290: E1048–E1056, 2006. First published December 20, 2005; doi:10.1152/ajpendo.00340.2005.—The partitioning of whole body carbon flux between fat and lean compartments affects body composition. We hypothesized that it is possible to simultaneously determine whole body carbon (energy) balance and the dynamics of lipids and proteins in specific tissues in vivo. Growing C57BL/6J mice fed a high-fat low-carbohydrate diet were injected with a bolus of “doubly labeled” water (i.e., <sup>2</sup>H<sub>2</sub>O and H<sub>2</sub><sup>18</sup>O). The rate of CO<sub>2</sub> production was determined from the difference between the elimination rates of <sup>2</sup>H and <sup>18</sup>O from body water. The rates of synthesis and degradation of triglycerides extracted from epididymal fat pads and of proteins extracted from heart muscle were determined by mathematically modeling the <sup>2</sup>H labeling of triglyceride-bound glycerol and protein-bound alanine, respectively. We found that mice were in positive carbon balance (~20% retention per day) and accumulated lipid in epididymal fat pads (~9 μmol triglyceride accumulated per day). This is consistent with the fact that mice were studied during a period of growth. Modeling the <sup>2</sup>H labeling of triglycerides revealed a substantial rate of lipid breakdown during this anabolic state (equivalent to ~25% of the newly synthesized triglyceride). We found equal rates of protein synthesis and breakdown in heart muscle (~10% of the pool per day), consistent with the fact that the heart muscle mass did not change. In total, these findings demonstrate a novel application of the doubly labeled water method. Utilization of this approach, especially in unique rodent models, should facilitate studies aimed at quantifying the efficacy of interventions that modulate whole body carbon balance and lipid flux while in parallel determining their impact on (cardiac) muscle protein turnover. Last, the simplicity of administering doubly labeled water and collecting samples allows this method to be used in virtually any laboratory setting.

metabolic regulation; carbon-energy balance; triglyceride turnover; protein turnover; stable isotope tracer kinetics

OBESITY PRESENTS A GLOBAL HEALTH CHALLENGE (20, 25), and many attempts are being made to determine the influence of environmental vs. genetic factors on the modeling of body composition. The application of isotope tracers in novel animal models offers a means of dissecting the importance of specific reactions on the pathogenesis and treatment of disease (12, 15).

We recently demonstrated the use of <sup>2</sup>H<sub>2</sub>O for measuring the turnover rates of triglycerides and proteins in vivo (3, 10, 24). Briefly, following the administration of <sup>2</sup>H<sub>2</sub>O, <sup>2</sup>H in body water equilibrates with the carbon-bound hydrogens of glycerol 3-phosphate and alanine. The rates of triglyceride and protein syntheses are determined by measuring the incorpora-

tion of the respective <sup>2</sup>H-labeled precursors into the appropriate end products. This simple and powerful method can be used in free-living subjects and complements other tracer methods for studying intermediary metabolism (12, 15, 18, 22, 36).

In our previous studies (3, 10, 24), rates of biochemical flux were determined under conditions of “steady-state” precursor labeling. Briefly, animals were given a bolus of <sup>2</sup>H<sub>2</sub>O and maintained on <sup>2</sup>H-labeled drinking water. The experimental design maintained a constant <sup>2</sup>H labeling of body water. Because kinetic parameters can be determined during conditions of non-steady-state precursor labeling, we hypothesized that it would be possible to measure lipid and protein dynamics after the administration of a bolus of <sup>2</sup>H<sub>2</sub>O. This modification offers a major advantage, since one can simultaneously administer a bolus of H<sub>2</sub><sup>18</sup>O and determine the rate of CO<sub>2</sub> production from the difference between the rates of elimination of <sup>2</sup>H and <sup>18</sup>O from body water (27, 36). We report here on a novel application of the “doubly labeled” water method. We demonstrate that by coupling the doubly labeled water method with measurements of <sup>2</sup>H incorporation into specific end products, it is possible to 1) estimate whole body carbon balance by comparing dietary intake and CO<sub>2</sub> production and 2) determine the rates of biochemical reactions that influence the modeling of lipids and proteins in specific tissues in vivo.

## MATERIALS AND METHODS

### Chemicals and Supplies

Unless specified, all chemicals and reagents were purchased from Sigma-Aldrich. <sup>2</sup>H<sub>2</sub>O (99.9 atom percent excess) and H<sub>2</sub><sup>18</sup>O (10.4 atom percent excess) were purchased from Cambridge Isotopes (Andover, MA) and Isotec (Miamisburg, OH), respectively. Ion exchange resins were purchased from Bio-Rad (Hercules, CA). GC-MS supplies were purchased from Agilent Technologies (Wilmington, DE) and Alltech (Deerfield, IL). Enzymes were purchased from Roche (Indianapolis, IN). Diets were purchased from Research Diets (New Brunswick, NJ). Mice were purchased from Jackson Laboratories (Bar Harbor, ME).

### Biological Experiments

On arrival, male C57BL/6J mice (5 wk old, *n* = 42) were fed a high-fat low-carbohydrate diet (no. D12451, kcal distribution equal to 45% fat, 35% carbohydrate, and 20% protein). After 5 days, mice were randomized into two groups, designated either “continuous” or “bolus,” and given an intraperitoneal injection of labeled water. Mice in the continuous group were injected with <sup>2</sup>H-labeled saline (20 μl/g body wt of 0.9 g NaCl in 1,000 ml 99% <sup>2</sup>H<sub>2</sub>O). After injection, mice were returned to their cages and maintained on 5% <sup>2</sup>H-labeled drinking water for 5 days before being switched to regular drinking

Address for reprint requests and other correspondence: S. F. Previs, Dept. of Nutrition, D-201, Case Western Reserve Univ. School of Medicine, Cleveland, OH 44106 (e-mail: stephen.previs@case.edu).

The costs of publication of this article were defrayed in part by the payment of page charges. The article must therefore be hereby marked “advertisement” in accordance with 18 U.S.C. Section 1734 solely to indicate this fact.

water. This procedure maintains a steady-state  $^2\text{H}$  labeling of body water at  $\sim 2.5\%$  (days 0–5), followed by an exponential elimination of the tracer from body water (after day 5), as previously described (3). Mice in the bolus group were injected with  $^2\text{H}$ - and  $^{18}\text{O}$ -labeled saline (40  $\mu\text{l/g}$  body wt of 0.9 g NaCl in 500 ml 99%  $^2\text{H}_2\text{O}$  + 500 ml 10%  $\text{H}_2^{18}\text{O}$ ). This will initially raise the body water enrichment to  $\sim 2.5$  and  $\sim 0.25\%$  of  $^2\text{H}$  and  $^{18}\text{O}$ , respectively. Mice in the bolus group were maintained on regular drinking water to allow for the exponential elimination of both  $^2\text{H}$  and  $^{18}\text{O}$  from body water. In all cases, to ensure the precision of the injection, mice were sedated by a brief exposure ( $\sim 15$  s) to Isoflurane (Baxter Pharmaceuticals, Deerfield, IL); mice regain consciousness within a minute with no apparent adverse side effects.

Mice in each group were fed ad libitum, and daily food consumption was measured. Mice were sedated on days 0, 2, 5, 7, 9, 12, and 15 postinjection ( $n = 3$  per day per group). Blood and tissue samples were collected and quick-frozen in liquid nitrogen. Samples were stored at  $-80^\circ\text{C}$  until analyses.

#### Generation of Positional Isotopomers of Glycerol 3-Phosphate

$^2\text{H}$  glycerol 3-phosphate standards were generated by reducing 100 mg of glyceraldehyde 3-phosphate or 100 mg of dihydroxyacetone phosphate with 75  $\mu\text{l}$  of  $\text{NaBD}_4$  solution (0.44 g  $\text{NaBD}_4/\text{ml}$  0.1 N NaOH). The reduction of glyceraldehyde 3-phosphate generated  $[1-^2\text{H}]$  glycerol 3-phosphate, and the reduction of dihydroxyacetone phosphate generated  $[2-^2\text{H}]$  glycerol 3-phosphate. The reaction was allowed to stand at room temperature for 1 h. Excess borodeuteride was destroyed by addition of 12 N HCl until the pH was acidic (pH  $\sim 1.0$ ). The sample was evaporated to dryness and then dissolved in 2.5 ml of 50% methanol-water (vol/vol). To remove methyl borate, the methanol-water was evaporated to dryness. The methanol-water treatment was repeated twice. The dry residues were dissolved in water and applied to AG 1-X8 ion exchange columns (formate form). The columns were first washed with 20 ml of water, and  $^2\text{H}$  glycerol 3-phosphates were then eluted in 20 ml of 4 N formic acid.

#### Analytic Procedures

**$^2\text{H}$  labeling of body water.** The  $^2\text{H}$  labeling of body water was determined by exchange with acetone (37). Briefly, 40  $\mu\text{l}$  of sample or standard were reacted with 2  $\mu\text{l}$  of 10 N NaOH and 4  $\mu\text{l}$  of a 5% (vol/vol) solution of acetone in acetonitrile for 24 h. Acetone was extracted by addition of 600  $\mu\text{l}$  of chloroform followed by addition of  $\sim 0.5$  g  $\text{Na}_2\text{SO}_4$ . Samples were vigorously mixed, and a small aliquot of the chloroform was transferred to a GC-MS vial.

Acetone was analyzed using an Agilent 5973N-MSD equipped with an Agilent 6890 GC system, and a DB-17MS capillary column (30 m  $\times$  0.25 mm  $\times$  0.25  $\mu\text{m}$ ) was used in all analyses. The temperature program was as follows:  $60^\circ\text{C}$  initial, increase by  $20^\circ\text{C}/\text{min}$  to  $100^\circ\text{C}$ , increase by  $50^\circ\text{C}/\text{min}$  to  $220^\circ\text{C}$ , and hold for 1 min. The sample was injected at a split ratio of 40:1 with a helium flow of 1 ml/min. Acetone eluted at  $\sim 1.5$  min. The mass spectrometer was operated in the electron impact mode (70 eV). Selective ion monitoring of mass-to-charge ratios ( $m/z$ ) 58 and 59 was performed using a dwell time of 10 ms per ion.

**$^{18}\text{O}$  labeling of body water.** The  $^{18}\text{O}$  labeling of body water was determined by conversion to trimethyl phosphate (TMP) (4). Briefly, TMP was generated by reacting phosphoric acid with diazomethane. All reactions were performed in a fume hood. The  $^{18}\text{O}$  enrichment was assayed as follows: 5  $\mu\text{l}$  of plasma sample or standard were added to a 12  $\times$  75-mm glass tube. To this,  $\sim 3$  mg of  $\text{PCl}_5$  were added to generate phosphoric acid, and samples were let stand for 20 min. Next, to the sample,  $\sim 300$   $\mu\text{l}$  of freshly prepared ethereal diazomethane were added, and the sample was allowed to stand until the ether evaporated. TMP was extracted by addition of 150  $\mu\text{l}$  of water and 600  $\mu\text{l}$  of chloroform followed by addition of  $\sim 0.5$  g  $\text{Na}_2\text{SO}_4$ . Samples were vigorously mixed, and a small aliquot of the chloroform

was transferred to a GC-MS vial. Note that, because diazomethane and its precursor are hazardous compounds, we generated diazomethane on a small scale, as needed. This was done by adding 2.5 ml of 40% KOH (wt/vol) and 8 ml of diethyl ether to a 20-ml scratch-free glass tube. To this, we added  $\sim 100$  mg of 1-methyl-3-nitro-1-nitrosoguanidine. The reaction was run until ether developed a dark green-yellow color. The ethereal diazomethane was used immediately to derivatize samples.

GC-MS analyses of TMP derivative were performed using the Agilent 5973N-MSD equipped with the Agilent 6890 GC system. A DB-17MS capillary column (30 m  $\times$  0.25 mm  $\times$  0.25  $\mu\text{m}$ ) was used in all analyses. The temperature program was  $90^\circ\text{C}$  initial, increase by  $30^\circ\text{C}/\text{min}$  to  $240^\circ\text{C}$ , and hold for 1 min. The split ratio was 20:1 with helium flow 1 ml/min. TMP eluted at  $\sim 2.4$  min. The  $^{18}\text{O}$  enrichment was determined using electron impact ionization (70 eV) and selected ion monitoring (10 ms dwell time) of  $m/z$  140 to 142. The  $^{18}\text{O}$  enrichment was calculated from the signal ratio  $(142)/(142 + 140)$ .

**$^2\text{H}$  labeling of triglyceride-bound glycerol.** Total glycerides were extracted from frozen epididymal fat pads by first hydrolyzing both fat pads in 1 N KOH-ethanol (20:80, vol/vol) at  $70^\circ\text{C}$ . After 3 h, the hydrolysate was evaporated to dryness, and dry residue was redissolved in 3 ml of  $\text{H}_2\text{O}$  and acidified to  $\sim \text{pH}$  1.0 by adding 6 N HCl. Free fatty acids were extracted using diethyl ether (3 times with 4 ml). The pH of the aqueous solution was then adjusted to  $\sim 7.0$  (using 10 N NaOH). Free glycerol was converted to glycerol 3-phosphate by incubating  $\sim 150$   $\mu\text{mol}$  of glycerol in 1.5 ml of Tris-EDTA buffer (pH 7.4) containing 0.2 M ATP and 5 U of glycerokinase for 2 h at  $37^\circ\text{C}$ .

Glycerol 3-phosphate was purified by passing the reaction mixture over an AG 1-X8 ion exchange resin (formate form). The column was first washed with 20 ml of water, and glycerol 3-phosphate was then recovered by washing with 20 ml of 4 N formic acid. The eluent containing glycerol 3-phosphate was evaporated to dryness and converted to its tetratrimethylsilyl derivative (G3P-TMS). This was done by reacting the dry glycerol 3-phosphate residue with 100  $\mu\text{l}$  of bis(trimethylsilyl) trifluoroacetamide + 10% trimethylchlorosilane (Regis, Morton Grove, IL) at  $75^\circ\text{C}$  for 30 min.

The  $^2\text{H}$  labeling of G3P-TMS was determined using the Agilent 5973N-MSD equipped with the Agilent 6890 GC system. A DB-17MS capillary column (30 m  $\times$  0.25 mm  $\times$  0.25  $\mu\text{m}$ ) was used in all analyses. The temperature program was  $120^\circ\text{C}$  initial, increase by  $10^\circ\text{C}/\text{min}$  to  $200^\circ\text{C}$ , increase by  $50^\circ\text{C}/\text{min}$  to  $240^\circ\text{C}$ , 2 min hold time. The split ratio was 40:1 with helium flow 1 ml/min. G3P-TMS eluted at  $\sim 8.0$  min. Electron impact ionization was used in all analyses. Selective ion monitoring of fragments  $m/z$  357 and 358 (containing carbons 2 and 3 and the respective carbon-bound hydrogens) and 445 and 446 (containing carbons 1, 2, and 3 and the respective carbon-bound hydrogens) was performed using a dwell time of 10 ms per ion (8).

Note that glycerol has biological asymmetry, and glycerokinase selectively phosphorylates carbon 3 (5, 26, 32). In this study, we determined the labeling of  $^2\text{H}$  that is bound to carbon 1 of triglyceride-glycerol from the difference of the molar percent enrichments (MPEs) of  $(358)/(357 + 358)$  and  $(446)/(445 + 446)$ ; i.e., the labeling of  $^2\text{H}$  bound to carbons 2 + 3 was subtracted from the labeling of  $^2\text{H}$  bound to carbons 1 + 2 + 3 (8). Calculations were based on the use of known standards of G3P-TMS.

**Concentration of triglyceride-bound glycerol.** The concentration of triglyceride-bound glycerol was determined by enzymatic/spectrophotometric assay. Briefly, epididymal fat pads were hydrolyzed, and free glycerol was obtained as described above. Glycerol was then redissolved in a known amount of Tris-EDTA buffer (pH 7.4) and its concentration determined using an enzymatic assay (Free Glycerol Reagent, Sigma).

**$^2\text{H}$  labeling of protein-bound alanine from heart muscle.** Hearts were homogenized in 10% (wt/vol) trichloroacetic acid (5 ml acid/g tissue). The protein pellet was washed three times with 5% trichloroacetic acid and then dissolved in 6 N HCl (5 ml/0.5 g tissue). The sample was reacted at  $100^\circ\text{C}$  for 18 h and then diluted 10-fold.

Alanine was then recovered following ion exchange chromatography. Briefly, samples were loaded onto an AG 50W-X8 ion exchange resin (hydrogen form), and the column was washed with 20 ml of H<sub>2</sub>O. Next, alanine was eluted by washing with 20 ml of 4 N NH<sub>3</sub>OH, and the NH<sub>3</sub>OH fraction was evaporated to dryness.

The <sup>2</sup>H labeling of alanine was determined on its methyl-8 derivative, formed by reaction with with *N,N*-dimethylformamide dimethylacetal (Pierce, Rockford, IL) (33). Samples were analyzed under electron impact ionization, the Agilent 5973N-MSD equipped with the Agilent 6890 GC system. A DB-17MS capillary column (30 m × 0.25 mm × 0.25 μm) was used in all analyses. The temperature program was 90°C initial, hold for 5 min, increase by 5°C/min to 130°C, increase by 40°C/min to 240°C, and hold for 5 min. The split ratio was 10:1 with a helium flow of 1 ml/min. Alanine eluted at ~12 min. The mass spectrometer was operated in the electron impact mode. Selective ion monitoring of the molecular ion was performed, i.e., *m/z* 158 and 159 (total <sup>2</sup>H labeling of alanine), using a dwell time of 10 ms per ion.

*Mathematical Model for Describing Triglyceride and Protein Kinetics*

*Steady-state isotope precursor labeling protocol.* Rates of synthesis and degradation of triglycerides and proteins were determined by fitting the concentration and <sup>2</sup>H labeling data (3). In the case of the continuous group (the steady-state <sup>2</sup>H labeling of body water), data were fitted as described (3). First, the concentration of triglyceride-bound glycerol or total protein is modeled. The incorporation of <sup>2</sup>H from water into lipids or proteins is modeled using a single-compartment model, assuming that the labeling of plasma water reflects that of water in adipose tissue and muscle, respectively. The time-dependent labeling of <sup>2</sup>H in water is *c(t)*. <sup>2</sup>H is eliminated from plasma at a rate *c'*. The parameters of basic interest, i.e., the rates of triglyceride or protein synthesis and degradation (*S* and *D*, respectively, expressed in units of mass per day), are estimated from the data using nonlinear least-squares fitting.

Because the mass of triglyceride (expressed in μmol) increased linearly with time (*m*, expressed in μmol per day), the total amount of labeled triglyceride at time *t* satisfies the differential equation

$$\frac{dh(t)}{dt} = Sc(t) - \frac{Dh(t)}{mt + b} \tag{1}$$

where *h* equals the <sup>2</sup>H labeling of triglyceride (expressed in μmol <sup>2</sup>H). The parameter *c(t)* is essentially constant while mice are maintained on <sup>2</sup>H-labeled drinking water, yet it decays exponentially (at *c'*) once mice are switched to regular water. The parameter *c'* is estimated from the data.

Differential Eq. 1 is then solved in closed form for the removal of <sup>2</sup>H-labeled drinking water. That equation is

$$v(t) = \frac{sc_0}{b + mt} \left\{ \frac{- \left[ b + mt \left( -1 + \frac{b}{b + mt} \right) \right]^{\frac{s}{m}}}{S} + \frac{(b + mt) \left( -1 + \frac{b + 5m}{b + mt} \right)^{\frac{s}{m}} \theta(t - 5)}{S} \right\} + \frac{sc_0}{b + mt} \left( a^{-\frac{s}{m}} e^{a \left( \frac{b}{m} + 5 \right)} \left( \frac{b}{m} + T \right)^{1 - \frac{s}{m}} \left\{ \Gamma \left[ \frac{S}{m}, \frac{a(b + 5m)}{m} \right] - \Gamma \left[ \frac{S}{m}, \frac{a(b + mt)}{m} \right] \theta(t - 5) \right\} \right) \tag{2}$$

where *c*<sub>0</sub> = *c*(0) and *v*<sub>0</sub> = *v*(0) represent the <sup>2</sup>H labeling (expressed in %enrichment) of body water and triglyceride-glycerol, respectively, at the time when <sup>2</sup>H<sub>2</sub>O is withdrawn, *θ* is the unit step function (0 for the negative argument and 1 for positive argument; this incorporates the change from enriched to unenriched water at *day 5*), *a* is the decay constant for labeled body water, and  $\Gamma(a, z)$  is the incomplete gamma function

$$\Gamma(a, z) = \int_z^\infty t^{a-1} e^{-t} dt. \tag{3}$$

The model was solved by using a linear least square fit of the data regarding the mass of triglycerides in adipose tissue. The only remaining parameters that require estimation are the rate of synthesis (*S*) and the rate of degradation (*D* = *S* - *m*). A Levenberg-Marquardt nonlinear fit (equal weights on all data points) is used to compute those parameters.

A similar approach was used to quantify protein dynamics in heart muscle. However, because the mass of the tissue remained constant during the course of the experiment, the term *m* is reduced to 0. Therefore, a modified differential equation is used, namely

$$\frac{dh(t)}{dt} = Sc(t) - \frac{Sh(t)}{b} \tag{4}$$

The data are then fitted using differential Eq. 4 and solving. The equation is

$$v(t) = c_0 \left\{ 1 - e^{-\frac{St}{b}} + \frac{[S - e^{-a(t-5)}S + a(e^{-\frac{S(t-5)}{b}} - 1)b]\theta(t - 5)}{ab - S} \right\} \tag{5}$$

*Non-steady-state isotope precursor labeling protocol.* Rates of synthesis and degradation of triglycerides and proteins were calculated from labeling data of mice that received a single bolus of <sup>2</sup>H<sub>2</sub>O (i.e., under the conditions of non-steady-state <sup>2</sup>H labeling of body water). As described above, the pool size was first modeled, followed by a fit of the <sup>2</sup>H labeling data. In the case of the bolus group, a new mathematical model was developed where *S* and *D* are estimated using the equation

$$v(t) = \frac{1}{m} \left[ a^{-\frac{s}{m}} c_0 e^{\frac{ab}{m}} S \left( \frac{b}{m} + t \right) - \frac{S}{m} \right] \Gamma \left( \frac{S}{m}, \frac{ab}{m} \right) - \Gamma \left[ \frac{S}{m}, a \left( \frac{b}{m} + t \right) \right] \tag{6}$$

for nonconstant total mass

$$v(t) = \frac{c_0 S (e^{-at} - e^{-\frac{St}{b}})}{S - ab} \tag{7}$$

and for constant total mass.

Note that, in all cases, the modeling assumes that the <sup>2</sup>H labeling of plasma water is the precursor. As discussed previously (3), each of the two hydrogens bound to carbon 1 of glycerol 3-phosphate is in equilibrium with water. Thus, when triglyceride dynamics are measured, the product labeling equals the total labeling of <sup>2</sup>H bound to carbon 1 of triglyceride-glycerol divided by 2. As discussed previously (10, 24), <sup>2</sup>H from body water is rapidly incorporated into virtually all of the four carbon-bound hydrogens of free alanine before alanine is incorporated into newly made proteins (<sup>2</sup>H equilibrates ~100% with the α-hydrogen and ~90% with each of the β-hydrogens). Thus, when protein dynamics are measured, the product labeling equals the total labeling of protein-alanine divided by 3.7. The best-fit solutions were determined and are stated as the rate ± the 95% confidence interval observed between the measured data and the model predictions.

*Calculations*

The rate of CO<sub>2</sub> production (mmol/day) was calculated using the equation

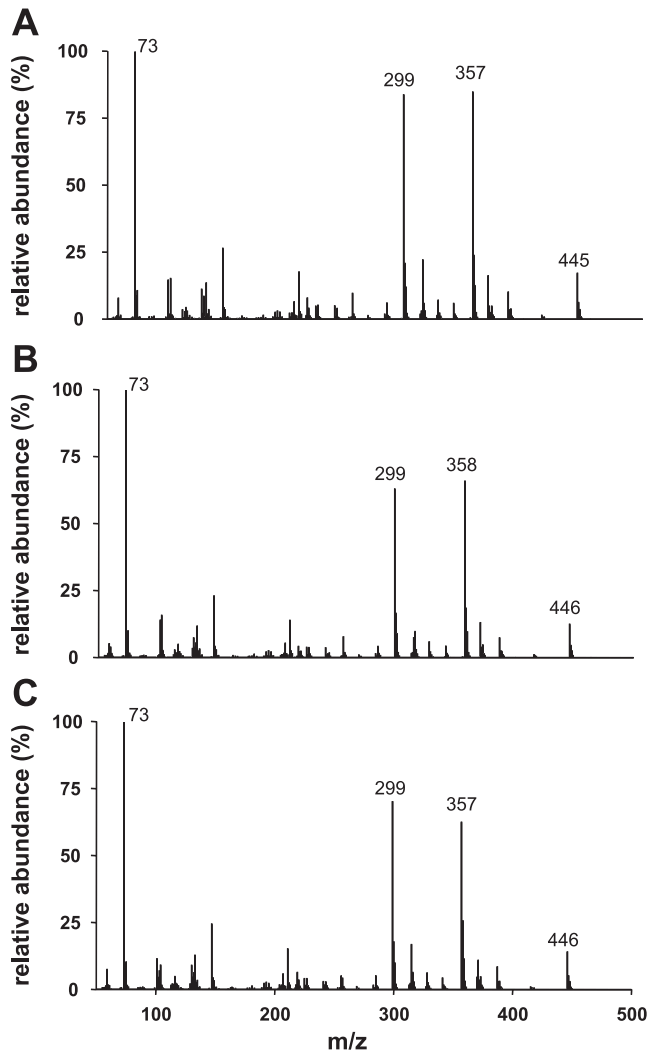


Fig. 1. Electron impact ionization mass spectra of *tetra*-trimethylsilyl glycerol 3-phosphate. Standards of glycerol 3-phosphate were either purchased (A) or generated by reducing commercially available dihydroxyacetone phosphate or glyceraldehyde 3-phosphate with sodium borodeuteride (B and C, respectively) and reacted to generate the respective *tetra*-trimethylsilyl derivatives. The absence of a true molecular ion at *m/z* 460 or 461 is consistent with the fragmentation pattern of trimethylsilyl derivatives. Shift in *m/z* 445 to 446 in B and C vs. A is expected, as *m/z* 445 (i.e., molecular ion minus 15 amu) contains all the carbon-bound hydrogens/deuteriums. Positional location of <sup>2</sup>H in B is on carbon 2 (dihydroxyacetone was reduced with sodium borodeuteride), whereas positional location of <sup>2</sup>H in C is on carbon 1 (glyceraldehyde 3-phosphate was reduced with sodium borodeuteride). Shift in *m/z* 357 to 358 (B vs. A) and lack of shift in *m/z* 357 to 358 (C vs. A) are consistent with the fact that *m/z* 357 contains carbons 2 + 3 and respective carbon-bound hydrogens/deuteriums.

$$\text{CO}_2 \text{ production} = \{(0.481 \times N) \times [(1.01 \times k^{18}\text{O}) - (1.04 \times k^2\text{H})] - (0.0246 \times 1.05 \times N \times (k^{18}\text{O} - k^2\text{H}))\} \quad (8)$$

where the fractional biological elimination constants (*k*<sup>18</sup>O and *k*<sup>2</sup>H, in days) are determined from the decrease in the labeling of body water and total body water (*N*, in mmol) is determined from the initial dilution of the tracers (i.e., the average pool size obtained from the dilution of each tracer) (28).

Unless noted, data are expressed as means ± SE.

RESULTS

<sup>2</sup>H from <sup>2</sup>H<sub>2</sub>O can be incorporated into five carbon-bound hydrogen positions of triglyceride-glycerol. We previously reported (3) that the rates of triglyceride synthesis and breakdown can be determined by measuring the labeling of <sup>2</sup>H that is bound to carbon 1 of triglyceride-glycerol divided by 2. In this study, we aimed to simplify our previous efforts for measuring the positional labeling of <sup>2</sup>H bound to carbon 1 of triglyceride-glycerol. Figure 1 shows the mass spectra of G3P-TMS. The fragment ion at *M* - 15 is typically observed with trimethylsilyl derivatives producing the molecular ion (*m/z* 460) minus a methyl group (*m/z* 445; Fig. 1A). The shift in *m/z* 445 to 446 is expected, since <sup>2</sup>H was incorporated during the reduction of the respective compounds with sodium borodeuteride (Fig. 1, A vs. B or C). The differential effect in shift observed at *m/z* 357 (to *m/z* 358) is consistent with the observations reported by Cronholm and Curstedt (8); i.e., the fragment ion at *m/z* 357 contains carbons 2 + 3 and their respective carbon-bound hydrogens (Fig. 1B, *m/z* 357 is shifted to *m/z* 358; Fig. 1C, no shift in *m/z* 357). The labeling of <sup>2</sup>H bound to carbon 1 of triglyceride-glycerol was determined by subtracting the labeling of <sup>2</sup>H bound to carbons 2 + 3 (*m/z* 357) from the labeling of <sup>2</sup>H bound to carbons 1 + 2 + 3 (*m/z* 445).

We were concerned that it would be difficult to obtain precise measurements of low <sup>2</sup>H enrichments of triglyceride-glycerol (~0.4 to 2% excess <sup>2</sup>H) since the background labeling in each fragment ion is relatively high; the chemical derivative contains silicon and carbon that have *M* + 1 isotopes equal to ~5 and ~1% of the predominant natural species, respectively (Fig. 1). Therefore, we examined the reproducibility of measurements of the background labeling in each fragment ion by means of repeated GC-MS measurements performed over several days (Table 1). Measurements were reproducible on an individual day; however, the measurements were somewhat variable over different days (Table 1).

Figure 2 demonstrates that mice gained weight (Fig. 2A: *y* = 0.295*x* + 18.9, *r*<sup>2</sup> = 0.99) and accumulated triglycerides in epididymal fat pads (Fig. 2B: *y* = 9.08*x* + 90.7, *r*<sup>2</sup> = 0.78; dashed lines represent 95% confidence interval). These data are

Table 1. Determination of intra- and interday reproducibility of measurements of *tetra*-trimethylsilyl glycerol 3-phosphate background labeling

Day	C1 + C2 + C3 446/(445 + 446)	C2 + C3 358/(357 + 358)	C1 (C1 + C2 + C3) - (C2 + C3)
1	26.08 ± 0.04 (CV 0.29%)	21.48 ± 0.01 (CV 0.14%)	4.60 ± 0.05 (CV 2.25%)
2	25.99 ± 0.01 (CV 0.10%)	21.59 ± 0.01 (CV 0.07%)	4.39 ± 0.01 (CV 0.48%)
3	26.03 ± 0.02 (CV 0.13%)	21.47 ± 0.02 (CV 0.15%)	4.56 ± 0.03 (CV 1.16%)

Data are expressed as means ± SE. CV, coefficient of variation for 5 replication determinations. Samples were assayed over various days using 5 injections per day. Abundance of 4 ion signals was measured, *m/z* 445 and 446 (containing carbons 1, 2, and 3 and respective carbon-bound hydrogens) and *m/z* 357 and 358 (containing carbons 2 and 3 and respective carbon-bound hydrogens). Data were tabulated as the natural mole percent in *M* + 1, i.e., the background labeling.

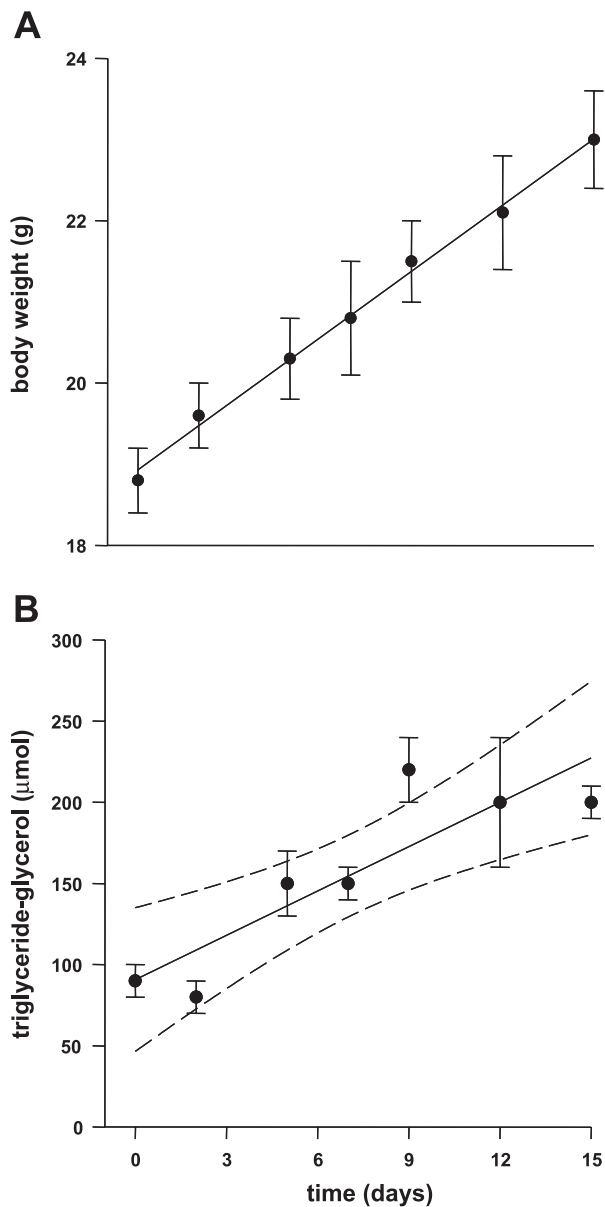


Fig. 2. Growth and lipid accretion in mice. Growing mice were fed a high-fat, low-carbohydrate diet for 15 days. Weight gain (A:  $y = 0.295x + 18.93$ ,  $r^2 = 0.99$ ) and lipid accretion (B:  $y = 9.08x + 90.7$ ,  $r^2 = 0.78$ ; dashed lines represent 95% confidence interval) were measured. As noted in MATERIALS AND METHODS, mice were randomized to 1 of 2 isotope labeling protocols. No differences were observed between mice randomized to either labeling protocol at similar time points; therefore, data from both groups were pooled ( $n = 42$  on day 0, 36 on day 2, 30 on day 5, 24 on day 7, 18 on day 9, 12 on day 12, and 6 on day 15). Data are expressed means  $\pm$  SE.

consistent with our previous observations (3). During the experimental period, there was no change in the wet weight of the hearts,  $142 \pm 9$  mg on day 0 vs.  $144 \pm 11$  mg on day 15 (consistent with unpublished observations).

Figure 3 shows the labeling profiles of body water, glycerol from total epididymal fat pad triglycerides, and alanine from total heart muscle proteins. While mice in the continuous group were maintained on  $^2\text{H}_2\text{O}$  (days 0–5), the  $^2\text{H}$  labeling of body water remained constant ( $2.59 \pm 0.10\%$   $^2\text{H}$ ) and equaled ~50% that of the drinking water, consistent with our previous

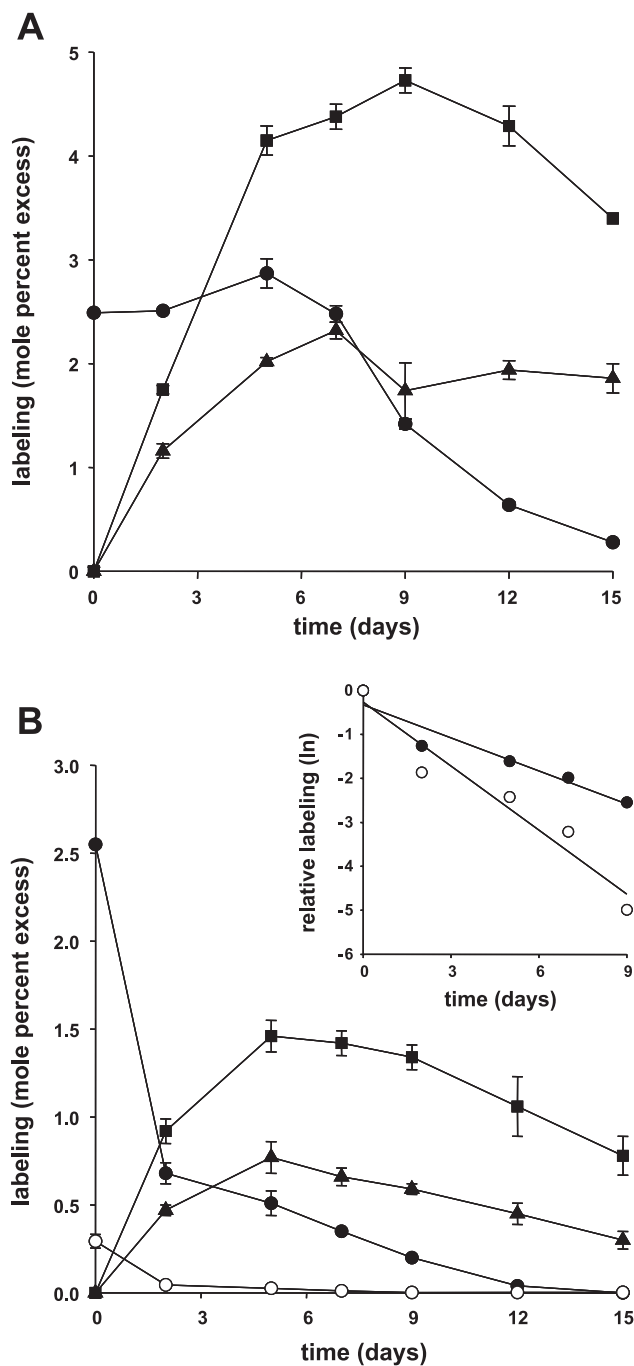


Fig. 3. Labeling of body water, glycerol from epididymal fat pad triglycerides, and alanine from heart muscle proteins. Mice were randomized to 1 of 2 isotope labeling protocols. A: “continuous” mice were maintained on  $^2\text{H}_2\text{O}$  for 5 days before being switched to regular drinking water. B: “bolus” mice were given a single injection containing a mixture of  $^2\text{H}_2\text{O}$  and  $\text{H}_2^{18}\text{O}$ .  $^2\text{H}$  enrichment of body water ( $\bullet$ ) and that bound to carbon 1 of triglyceride-glycerol ( $\blacktriangle$ ) and protein-alanine ( $\blacksquare$ ) were determined (A and B). In addition,  $^{18}\text{O}$  labeling of body water ( $\circ$ ) was determined (B). Data are expressed as total labeling measured in each species. Inset: labeling of  $^2\text{H}$  and  $^{18}\text{O}$  of body water (normalized against labeling on day 0 and expressed in natural log scale). Elimination rates of  $^2\text{H}$  and  $^{18}\text{O}$  were determined from the slopes of regression analyses ( $^2\text{H}$  elimination:  $y = -0.248x$ ,  $r^2 = 0.901$ ;  $^{18}\text{O}$  elimination:  $y = -0.485x$ ,  $r^2 = 0.941$ ).

observations.  $^2\text{H}$  was eliminated from body water by switching mice from  $^2\text{H}$ -labeled drinking water to regular water (days 6–15). The  $^2\text{H}$  enrichment of body water decayed exponentially to  $\sim 0.28\%$  on day 15. The  $t_{1/2}$  of body water, calculated from the elimination rate of  $^2\text{H}$ , was  $\sim 2.3$  days. Again, this is consistent with our previous observations. The elimination of  $^2\text{H}$  from body water of mice in the bolus group (Fig. 3B:  $t_{1/2}$  of  $^2\text{H}$   $\sim 2.8$  days) was similar to that observed in mice in the continuous group. As expected, the elimination of  $^{18}\text{O}$  from body water was greater than that of  $^2\text{H}$  (Fig. 3B:  $t_{1/2}$  of  $^{18}\text{O}$   $\sim 1.4$  days). The calculated rate of  $\text{CO}_2$  production was  $\sim 74$  mmol/day.

Figure 4 shows the best fits of the mathematical models that were used to describe the  $^2\text{H}$  labeling of triglyceride-glycerol and protein-alanine. The calculated rates of synthesis and breakdown of triglycerides were  $12.6 \pm 1.4$  and  $3.8 \pm 1.4$  vs.  $12.9 \pm 2.8$  and  $4.1 \pm 2.8$   $\mu\text{mol}/\text{day}$ , using the steady-state vs. the non-steady-state labeling protocol (Fig. 4, A vs. B, respectively). The data obtained from mice in the continuous group (Fig. 4A) agree with previously published data (3). The good agreement between the two labeling protocols supports the use of the non-steady-state model (Fig. 4, A vs. B). Also, these data are consistent with the observation that high-fat feeding promotes lipid accretion. As there was no change in the wet weight of the hearts, modeling the  $^2\text{H}$  labeling of protein-bound alanine yields equal rates of synthesis and breakdown of total cardiac protein with respect to each protocol, i.e.,  $14.4 \pm 1.1$  vs.  $14.1 \pm 1.0$  mg wet wt/day, using the steady-state vs. the non-steady-state labeling protocol (Fig. 4, C and D, respectively). Overall, there was good agreement between the two labeling protocols.

## DISCUSSION

Isotope tracers can be used to quantify the turnover rates of various intermediates and yield information regarding metabolic regulation (18, 22, 36, 38). However, studies often consider either one nutritional state (e.g., fed or fasted) and/or examine one component of a problem (e.g., measure lipid or protein dynamics). In that regard, the doubly labeled water method is a unique tracer method because it yields an integrative measurement of total energy expenditure, including basal metabolism, thermic effect of eating, and physical activity (16, 17, 19). In this report, we demonstrate a novel application of the doubly labeled water method; i.e., after the administration of a bolus containing  $^2\text{H}_2\text{O}$  and  $\text{H}_2^{18}\text{O}$ , it is possible to measure the  $^2\text{H}$  labeling of lipids and proteins and thereby determine their rates of synthesis and degradation in vivo. Implementation of this approach required the development of a mathematical model to determine kinetic parameters under conditions of “non-steady-state” isotope precursor labeling. To further enhance the utilization of our method, we developed a simple GC-MS method for measuring the positional  $^2\text{H}$  labeling of triglyceride-glycerol. In discussing our observations, we first comment on the analytic developments, and second we comment on the biological outcomes of the study.

### Improving the Analytical Method for Measuring the $^2\text{H}$ Labeling of Triglyceride-Glycerol

The rate of triglyceride turnover is determined by measuring the labeling of  $^2\text{H}$  bound to carbon 1 of triglyceride-glycerol divided by 2 (the number of exchangeable hydrogens) (3). Previously, those measurements were made using the “hexa-

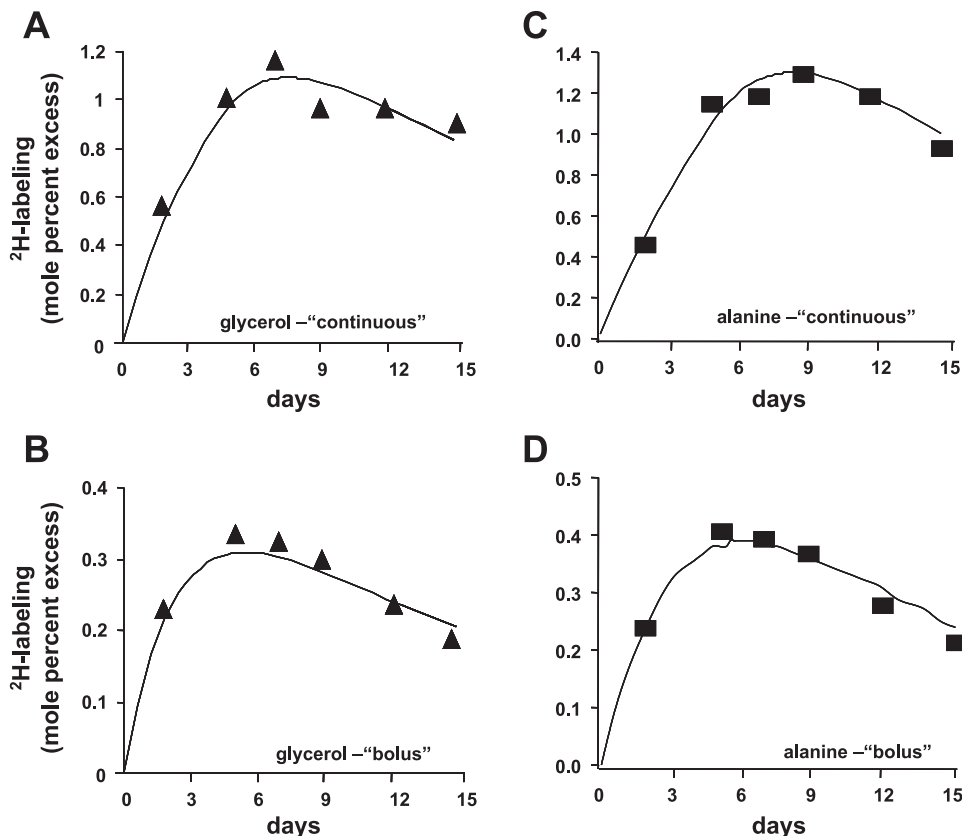


Fig. 4. Best fit of  $^2\text{H}$  labeling of glycerol from epididymal fat pad triglycerides and alanine from heart muscle proteins. Mathematical models were used to fit  $^2\text{H}$  labeling of glycerol and alanine isolated from epididymal fat pad triglycerides and heart muscle proteins, respectively. A and C: best fit of data obtained from mice in continuous group. B and D: best fit of data obtained from mice in bolus group. Virtually identical rates of synthesis and degradation of triglycerides were obtained using either protocol: A  $12.6 \pm 1.4$  and  $3.8 \pm 1.4$  vs. B  $12.9 \pm 2.8$  and  $4.1 \pm 2.8$   $\mu\text{mol}/\text{day}$ , using the steady-state vs. the non-steady-state labeling protocol, respectively. Also, modeling the  $^2\text{H}$  labeling of protein-bound alanine yielded equal rates of synthesis and degradation regardless of the protocol: C  $14.4 \pm 1.1$  vs. D  $14.1 \pm 1.0$  mg wet wt/day, using the steady-state vs. the non-steady-state labeling protocol. Note: scales used on the y-axis are different in Figs. 3 and 4. Data are modeled using a precursor-to-product labeling ratio, where the precursor is  $^2\text{H}$  labeling of body water and the product is labeling of  $^2\text{H}$  bound to carbon 1 of triglyceride-glycerol divided by 2 and labeling of  $^2\text{H}$  bound to total protein-bound alanine divided by 3.7 (no. of exchangeable hydrogens in the respective products); see MATERIALS AND METHODS.

methylenetetramine method" (6, 13). Although novel and effective, the hexamethylenetetramine method requires HPLC equipment and a manually operated distillation apparatus. The former makes the method costly, and the latter makes the method less than ideal when large numbers of samples are processed.

Because improving the analytic throughput should facilitate the use of  $^2\text{H}_2\text{O}$  for measuring triglyceride kinetics, we examined the applicability of a GC-MS method for measuring the positional labeling of triglyceride-glycerol (8). Our concern was to obtain reliable measurements of low  $^2\text{H}$  enrichment over a relatively high background; e.g., in the current study, biological samples were enriched  $\sim 0.4\text{--}2.0\%$  excess  $^2\text{H}$  over  $\sim 20\text{--}26\%$  background labeling (Fig. 3). The high background (Table 1) is a consequence of the fact that the trimethylsilyl derivative of glycerol 3-phosphate contains silicon and carbon, which have  $M + 1$  isotopes of  $\sim 5$  and  $\sim 1\%$ , respectively, of the predominant natural species. We found that the overall GC-MS method has good precision; i.e., the average coefficient of variation for measuring the background labeling of carbon 1 is  $\sim 1.3\%$  (Table 1). Because the average background labeling of carbon 1 is  $\sim 4.5\%$ , one can expect  $\sim 0.06\%$  absolute variation in the measurements (i.e.,  $4.5 \times 0.013$ ).

It is clear from Table 1 that GC-MS analyses of glycerol 3-phosphate labeling have rather poor accuracy, the absolute interdaily variation in background labeling ranging over  $\sim 0.2\%$  (Table 1). Therefore, it is not possible to reliably determine the  $^2\text{H}$  labeling by use of a theoretical model, i.e., by correcting the natural background from experimental samples (36). Consequently, we generated  $^2\text{H}$ -labeled standards by reducing commercially available glyceraldehyde 3-phosphate and dihydroxyacetone phosphate with sodium borodeuteride (Fig. 1). These standards offer two advantages. First, the analyses of known standards account for daily variations in the performance of the GC-MS instrument. Second, it is possible to amplify the detection of  $^2\text{H}$  labeling by integrating the leading edge of a chromatographic peak; i.e., biasing the ion chromatogram integration routine enhances the detection of  $^2\text{H}$  labeling (14).

It should be noted that other investigators are using  $^2\text{H}_2\text{O}$  to study triglyceride turnover (7, 34). It appears that the primary difference between the views expressed herein and those of Hellerstein and colleagues centers on how one defines/determines the product labeling (7, 34). It seems that they believe that it is sufficient to use a statistical method to determine the equilibrium of label incorporation in a product molecule, whereas we have used analytical methods to measure the labeling of specific hydrogen atoms in a product molecule. It may be that in certain instances the same results (regarding biochemical flux) will be obtained regardless of how the product labeling is defined. Examining the latter point is an area of ongoing research by our laboratory, especially since using the total product labeling increases the sensitivity of the measurements (see below).

#### *Advantage of Non-Steady-State Isotope Precursor Labeling*

Approximately 50 years ago, Lifson and colleagues (16, 17) demonstrated the use of the doubly labeled water method for determining rates of  $\text{CO}_2$  production in vivo. Since those pioneering studies, investigators have refined and extended the

method to measure  $\text{CO}_2$  production in various species, including humans (27, 36). We hypothesized that it would be possible to further extend the doubly labeled water method and determine the flux of metabolic pathways by measuring the  $^2\text{H}$  labeling of certain biochemical end products. Our hypothesis was formulated on the classical studies of Schoenheimer and Rittenberg performed  $\sim 80$  years ago (30). Validation of this non-steady-state approach was performed against tracer studies in which a "steady-state" precursor was maintained.

Rates of  $\text{CO}_2$  production were calculated from the difference between the elimination rates of  $^2\text{H}$  and  $^{18}\text{O}$  from the body water (Fig. 3B, *inset*). We determined that mice produce  $\sim 74$  mmol of  $\text{CO}_2$  per day. On comparing the rate of  $\text{CO}_2$  production against the food intake ( $\sim 93$  mmol carbon per day), we found that mice retained  $\sim 20\%$  of the carbon intake. Although it is beyond the scope of this investigation to calculate the exact carbon balance (e.g., metabolic cages are needed to collect nonabsorbed food and/or solid waste), our findings are in strong agreement with the original studies of McClintock and Lifson (19). For example, in our study, mice were fed a high-fat diet and gained  $\sim 295$  mg body wt per day (Fig. 2). This is comparable to the gains reported by McClintock and Lifson; i.e., control mice retained  $\sim 9\%$  of total caloric intake and gained  $\sim 200$  mg body wt per day, and obese hyperphagic mice retained  $\sim 20\%$  of total caloric intake and gained  $\sim 429$  mg body wt per day (19).

Because C57BL/6J mice are sensitive to diet-induced obesity via high-fat feeding (23), we expected to observe lipid accretion (Fig. 2B). Regardless of the labeling protocol, we observed similar and substantial rates of incorporation of  $^2\text{H}$  into triglyceride-glycerol (Fig. 3, A and B). Despite the fact that the  $^2\text{H}$  labeling of triglyceride-glycerol is about three- to fivefold lower in the bolus group compared with the continuous group (Fig. 3), we observed strong agreement between the rates of triglyceride synthesis and degradation in both protocols (Fig. 4). This demonstrates the robust nature of these protocols and the reproducibility of the analyses.

The observation of a substantial rate of triglyceride breakdown (equivalent to  $\sim 25\%$  the rate of triglyceride synthesis) during lipid accretion is especially intriguing. This clearly demonstrates that adipose tissue is a highly active storage site and not simply an inert depot of triglycerides. Our observation is consistent with the conclusions drawn by Schoenheimer and Rittenberg (29) and substantiates the recent hypothesis proposed by Frayn et al. (11). Finally, it should be noted that, by measuring the  $^2\text{H}$  labeling of triglyceride-bound fatty acids, it is possible to determine the contribution of de novo lipogenesis to the source of fatty acids used in triglyceride synthesis (not shown) (1, 3, 9).

Considering the current problem of obesity (20, 25), and since cardiac failure has been observed in cases of rapid weight loss (2, 35), we anticipate that future studies may need to examine whether therapeutic interventions (e.g., dietary, pharmacological, or surgical) that are designed to affect lipid accretion also affect protein turnover, especially in the heart. Consequently, we determined whether it would be possible to measure the rates of protein turnover while measuring lipid flux. By mathematically modeling the  $^2\text{H}$  labeling of protein-bound alanine, we were able to derive rates of protein synthesis and protein breakdown in the heart muscle (Fig. 3). We found that a best fit of the data yielded virtually identical rates of

protein synthesis and breakdown (Fig. 4). This should be expected, as the mass of the heart muscle did not change over the study period.

It should be noted that, although we determined protein turnover only in heart muscle,  $^2\text{H}_2\text{O}$  can be used to study the turnover of proteins in different tissues, the requirement being that one needs to isolate the tissues and/or proteins of interest (10, 24). Also, we (31) recently demonstrated that it is possible to measure the turnover of specific proteins without extensive purification by coupling the administration of  $^2\text{H}_2\text{O}$  with proteomic-based assays. Thus, in theory, one can readily quantify the synthesis and degradation of individual components of the proteome.

### Summary and Conclusions

In summary,  $^2\text{H}$ - and  $^{18}\text{O}$ -labeled water can be used to quantify the contribution of anabolic and catabolic mechanisms that influence the dynamics of lipids and proteins.  $^2\text{H}_2\text{O}$  appears to be a particularly good tracer to use under conditions of non-steady-state isotope precursor labeling. First, because  $^2\text{H}$  rapidly distributes and equilibrates in body water, compartmentalization is not a major concern. Second, because body water has a relatively long half-life, there is a substantial amount of time for incorporation of  $^2\text{H}$  into slow-turning pools of macromolecules (e.g., triglycerides and proteins). Third, the elimination of  $^2\text{H}$  from body water follows a single exponential decay and occurs at a relatively slow rate, which facilitates measurements of  $^2\text{H}$  labeling.

We conclude that it is possible to extend the application of the doubly labeled water method and obtain measurements of  $\text{CO}_2$  production and the tissue-specific dynamics of lipids and proteins in vivo. As the methods presented here can be applied in any animal resource center/laboratory, our approach should complement the existing tools for studying metabolic regulation, e.g., the hyperinsulinemic euglycemic clamp (12, 15). In particular, virtually no surgical expertise is required to administer doubly labeled water and collect tissue samples. Also, the analytical methods require a minimum of relatively common, high-throughput, gas chromatography-electron impact ionization-mass spectrometry equipment. Finally, although we have measured the incorporation of  $^2\text{H}$  into two classes of macromolecules (lipids and proteins), presumably one could study the dynamics of other important end products, e.g., DNA (21).

### GRANTS

This work was supported by the National Institutes of Health (training fellowships 2T32 HL-007653-16A1 to I. R. Bederman and DK-007319 to D. A. Dufner and RoadMap 1R33 DK-070291-01), the Mt. Sinai Health Care Foundation (Cleveland, OH), and an unrestricted research grant from Merck Pharmaceuticals (Rahway, NJ).

### REFERENCES

1. Bassilian S, Ahmed S, Lim SK, Boros LG, Mao CS, and Lee WN. Loss of regulation of lipogenesis in the Zucker diabetic rat. II. Changes in stearate and oleate synthesis. *Am J Physiol Endocrinol Metab* 282: E507–E513, 2002.
2. Brown JM, Yetter JF, Spicer MJ, and Jones JD. Cardiac complications of protein-sparing modified fasting. *JAMA* 240: 120–122, 1978.
3. Brunengraber DZ, McCabe BJ, Kasumov T, Alexander JC, Chandramouli V, and Previs SF. Influence of diet on the modeling of adipose tissue triglycerides during growth. *Am J Physiol Endocrinol Metab* 285: E917–E925, 2003.
4. Brunengraber DZ, McCabe BJ, Katanik J, and Previs SF. Gas chromatography-mass spectrometry assay of the ( $^{18}\text{O}$ ) enrichment of water as trimethyl phosphate. *Anal Biochem* 306: 278–282, 2002.
5. Bulbitz C and Kennedy EP. A note on the asymmetrical metabolism of glycerol. *J Biol Chem* 211: 963–967, 1954.
6. Chandramouli V, Ekberg K, Schumann WC, Kalhan SC, Wahren J, and Landau BR. Quantifying gluconeogenesis during fasting. *Am J Physiol Endocrinol Metab* 273: E1209–E1215, 1997.
7. Chen JL, Peacock E, Samady W, Turner SM, Neese RA, Hellerstein MK, and Murphy EJ. Physiologic and pharmacologic factors influencing glyceroneogenic contribution to triacylglyceride glycerol measured by mass isotopomer distribution analysis. *J Biol Chem* 280: 25396–25402, 2005.
8. Cronholm T and Curstedt T. Heterogeneity of the sn-glycerol 3-phosphate pool in isolated hepatocytes, demonstrated by the use of deuterated glycerols and ethanol. *Biochem J* 224: 731–739, 1984.
9. Diraison F, Pachiardi C, and Beylot M. Measuring lipogenesis and cholesterol synthesis in humans with deuterated water: use of simple gas chromatographic/mass spectrometric techniques. *J Mass Spectrom* 32: 81–86, 1997.
10. Dufner DA, Bederman IR, Brunengraber DZ, Rachdaoui N, Ismail-Beigi F, Siegfried BA, Kimball SR, and Previs SF. Using  $^2\text{H}_2\text{O}$  to study the influence of feeding on protein synthesis: effect of isotope equilibration in vivo vs. in cell culture. *Am J Physiol Endocrinol Metab* 288: E1277–E1283, 2005.
11. Frayn KN. Adipose tissue as a buffer for daily lipid flux. *Diabetologia* 45: 1201–1210, 2002.
12. Fueger PT, Shearer J, Bracy DP, Posey KA, Pencek RR, McGuinness OP, and Wasserman DH. Control of muscle glucose uptake: test of the rate-limiting step paradigm in conscious, unrestrained mice. *J Physiol* 562: 925–935, 2005.
13. Jensen MD, Chandramouli V, Schumann WC, Ekberg K, Previs SF, Gupta S, and Landau BR. Sources of blood glycerol during fasting. *Am J Physiol Endocrinol Metab* 281: E998–E1004, 2001.
14. Katanik J, McCabe BJ, Brunengraber DZ, Chandramouli V, Nishiyama FJ, Anderson VE, and Previs SF. Measuring gluconeogenesis using a low dose of  $^2\text{H}_2\text{O}$ : advantage of isotope fractionation during gas chromatography. *Am J Physiol Endocrinol Metab* 284: E1043–E1048, 2003.
15. Kim JK, Michael MD, Previs SF, Peroni OD, Mauvais-Jarvis F, Neschen S, Kahn BB, Kahn CR, and Shulman GI. Redistribution of substrates to adipose tissue promotes obesity in mice with selective insulin resistance in muscle. *J Clin Invest* 105: 1791–1797, 2000.
16. Lifson N, Gordon GB, and McClintock R. Measurement of total carbon dioxide production by means of  $\text{D}_2\text{O}^{18}$ . *J Appl Physiol* 7: 704–710, 1955.
17. Lifson N and McClintock R. Theory of use of the turnover rates of body water for measuring energy and material balance. *J Theoret Biol* 12: 46–74, 1966.
18. McCabe BJ and Previs SF. Using isotope tracers to study metabolism: application in mouse models. *Metab Eng* 6: 25–35, 2004.
19. McClintock R and Lifson N.  $\text{CO}_2$  output and energy balance of hereditary obese mice. *Am J Physiol* 189: 463–469, 1957.
20. Mokdad AH, Serdula MK, Dietz WH, Bowman BA, Marks JS, and Koplan JP. The spread of the obesity epidemic in the United States, 1991–1998. *JAMA* 282: 1519–1522, 1999.
21. Neese RA, Misell LM, Turner S, Chu A, Kim J, Cesar D, Hoh R, Antelo F, Strawford A, McCune JM, Christiansen M, and Hellerstein MK. Measurement in vivo of proliferation rates of slow turnover cells by  $^2\text{H}_2\text{O}$  labeling of the deoxyribose moiety of DNA. *Proc Natl Acad Sci USA* 99: 15345–15350, 2002.
22. Patterson BW. Use of stable isotopically labeled tracers for studies of metabolic kinetics: an overview. *Metabolism* 46: 322–329, 1997.
23. Petro AE, Cotter J, Cooper DA, Peters JC, Surwit SJ, and Surwit RS. Fat, carbohydrate, and calories in the development of diabetes and obesity in the C57BL/6J mouse. *Metabolism* 53: 454–457, 2004.
24. Previs SF, Fatica R, Chandramouli V, Alexander JC, Brunengraber H, and Landau BR. Quantifying rates of protein synthesis in humans by use of  $^2\text{H}_2\text{O}$ : application to patients with end-stage renal disease. *Am J Physiol Endocrinol Metab* 286: E665–E672, 2004.
25. Rocchini AP. Childhood obesity and a diabetes epidemic. *N Engl J Med* 346: 854–855, 2002.
26. Schambye P and Wood HG. Biological asymmetry of glycerol and formation of asymmetrically labeled glucose. *J Biol Chem* 206: 875–882, 1954.
27. Schoeller DA. Measurement of energy expenditure in free-living humans by using doubly labeled water. *J Nutr* 118: 1278–1289, 1988.



28. **Schoeller DA, Ravussin E, Schutz Y, Acheson KJ, Baertschi P, and Jéquier E.** Energy expenditure by doubly labeled water: validation in humans and proposed calculation. *Am J Physiol Regul Integr Comp Physiol* 250: R823–R830, 1986.
29. **Schoenheimer R and Rittenberg D.** Deuterium as an indicator in the study of intermediary metabolism. III. The role of the fat tissues. *J Biol Chem* 111: 175–181, 1935.
30. **Schoenheimer R and Rittenberg R.** The study of intermediary metabolism of animals with the aid of isotopes. *Physiol Rev* 20: 218–248, 1940.
31. **Sun G, Wang B, Previs SF, and Anderson VE.** Simultaneous determination of multiple protein synthesis rates by in vivo deuterium labeling. *J Am Soc Mass Spec* 15: 92S, 2004.
32. **Swick RW and Nakao A.** The biological asymmetry of glycerol. *J Biol Chem* 206: 883–886, 1954.
33. **Thenot JP and Horning EC.** Amino acid N-dimethylaminomethylene alkyl esters. New derivatives for gas chromatographic and gas chromatographic-mass spectrometric studies. *Anal Lett* 5: 519–529, 1972.
34. **Turner SM, Murphy EJ, Neese RA, Antelo F, Thomas T, Agarwal A, Go C, and Hellerstein MK.** Measurement of TG synthesis and turnover in vivo by  $^2\text{H}_2\text{O}$  incorporation into the glycerol moiety and application of MIDA. *Am J Physiol Endocrinol Metab* 285: E790–E803, 2003.
35. **Vertes V, Genuth SM, and Hazelton IM.** Precautions with supplemented fasting. *JAMA* 238: 2142, 1977.
36. **Wolfe RR and Chinkes DL.** *Isotope Tracers in Metabolic Research: Principles and Practice of Kinetic Analyses.* New York: Wiley-Liss, 2004.
37. **Yang D, Diraison F, Beylot M, Brunengraber DZ, Samols MA, Anderson VE, and Brunengraber H.** Assay of low deuterium enrichment of water by isotopic exchange with [U- $^{13}\text{C}$ ]acetone and gas chromatography-mass spectrometry. *Anal Biochem* 258: 315–321, 1998.
38. **Zak R, Martin AF, and Blough R.** Assessment of protein turnover by use of radioisotopic tracers. *Physiol Rev* 59: 407–447, 1979.

